Published in final edited form as:
Neuroscience. 2005 ; 130(4): 1069–1081. doi:10.1016/j.neuroscience.2004.10.028.

CHOLINERGIC NEUROTRANSMISSION IN THE PREBÖTZINGER COMPLEX MODULATES EXCITABILITY OF INSPIRATORY NEURONS AND REGULATES RESPIRATORY RHYTHM

X. M. SHAO[*] and **J. L. FELDMAN**
Department of Neurobiology, David Geffen School of Medicine at UCLA, Box 951763, Los Angeles, CA 90095-1763, USA

Abstract

We investigated whether there is endogenous acetylcholine (ACh) release in the preBötzinger Complex (preBötC), a medullary region hypothesized to contain neurons generating respiratory rhythm, and how endogenous ACh modulates preBötC neuronal function and regulates respiratory pattern. Using a medullary slice preparation from neonatal rat, we recorded spontaneous respiratory-related rhythm from the hypoglossal nerve roots (XIIn) and patch-clamped preBötC inspiratory neurons. Unilateral mi-croinjection of physostigmine, an acetylcholinesterase inhibitor, into the preBötC increased the frequency of respiratory-related rhythmic activity from XIIn to 116±13% (mean±S.D.) of control. Ipsilateral physostigmine injection into the hypoglossal nucleus (XII nucleus) induced tonic activity, increased the amplitude and duration of the integrated inspiratory bursts of XIIn to 122±17% and 117±22% of control respectively; but did not alter frequency. In pre-BötC inspiratory neurons, bath application of physostigmine (10 μM) induced an inward current of 6.3±10.6 pA, increased the membrane noise, decreased the amplitude of phasic inspiratory drive current to 79±16% of control, increased the frequency of spontaneous excitatory postsynaptic currents to 163±103% and decreased the whole cell input resistance to 73±22% of control without affecting the threshold for generation of action potentials. Bath application of physostigmine concurrently induced tonic activity, increased the frequency, amplitude and duration of inspiratory bursts of XIIn motor output. Bath application of 4-diphenylacetoxy-*N*-methylpiperidine methiodide (4-DAMP, 2 μM), a M3 muscarinic acetylcholine receptor (mAChR) selective antagonist, increased the input resistance of preBötC inspiratory neurons to 116±9% of control and blocked all of the effects of physostigmine except for the increase in respiratory frequency. Dihydro-β-erythroidine (DH-β-E; 0.2 μM), an α4β2 nicotinic receptor (nAChR) selective antagonist, blocked all the effects of physostigmine except for the increase in inspiratory burst amplitude. In the presence of both 4-DAMP and DH-β-E, physostigmine induced opposite effects, i.e. a decrease in frequency and amplitude of XIIn rhythmic activity. These results suggest that there is cholinergic neurotransmission in the preBötC which regulates respiratory frequency, and in XII nucleus which regulates tonic activity, and the amplitude and duration of inspiratory bursts of XIIn in neonatal rats. Physiologically relevant levels of ACh release, via mAChRs antagonized by 4-DAMP and nAChRs antagonized by DH-β-E, modulate the excitability of

[*]Corresponding author. Tel: +1-310-825-1586; fax: +1-310-825-2224. mshao@ucla.edu (X. M. Shao).

inspiratory neurons and excitatory neurotransmission in the preBötC, consequently regulating respiratory rhythm.

Keywords

respiratory regulation; acetylcholine; muscarinic receptor; nicotinic receptor; physostigmine; medullary slice

Cholinergic neurotransmission is integral to a variety of brain functions including regulation of breathing. Physostigmine intravenously infused in rabbits increases respiratory rate, probably by raising the concentration of acetylcholine (ACh) in the central nervous system (CNS) (Weinstock et al., 1981). Application of physostigmine to the en bloc brainstem–spinal cord preparation from the neonatal rat (Smith and Feldman, 1987) increases respiratory frequency and potentiates the frequency increase resulting from exogenous application of ACh (Monteau et al., 1990). Inhibition of ACh release by vesamicol or cetiedil depresses respiratory motor output in the en bloc brainstem–spinal cord preparation (Burton et al., 1994). Muscarinic acetylcholine receptors (mAChRs) and nicotinic acetylcholine receptors (nAChRs) are present in medullary respiratory-related regions including the rostroventrolateral medulla and the hypoglossal nucleus (XII nucleus; Wada et al., 1989; Nattie and Li, 1990; Levey et al., 1991; Dominguez del Toro et al., 1994; Mallios et al., 1995; Chamberlin et al., 2002; Robinson et al., 2002; Dehkordi et al., 2004). Exogenously applied muscarine increases respiratory frequency and amplitude and duration of respiratory-related hypoglossal nerve root (XIIn) rhythmic activity by acting on M3-like mAChRs, modulating the excitability of preBötC neurons (Shao and Feldman, 2000). Application of nicotinic agonists modulates excitatory neurotransmission in the preBötzinger complex (preBötC) and regulates respiratory frequency and pattern; these effects can be completely blocked by dihydro-β-erythroidine (DH-β-E; Shao and Feldman, 2001, 2002). However, little is known about how endogenous ACh release modulates neuronal function in the preBötC, an essential site for respiratory rhythm generation in mammals (Smith et al., 1991; Feldman et al., 2003), and how it regulates respiratory frequency and pattern.

Brainstem cholinergic systems are postulated to play a role in pathological conditions related to central control of breathing such as sudden infant death syndrome (Kinney et al., 1995; Mallard et al., 1999) and sleep disordered breathing (sleep apnea; Bellingham and Ireland, 2002; Chamberlin et al., 2002; Gilman et al., 2003). ACh in brainstem regions associated with sleep is involved in state-dependent respiratory depression (Lydic and Baghdoyan, 1993). Central respiratory depression is a critical factor underlying fatal respiratory failure during organo-phosphate poisoning by nerve gases or agricultural insecticides (Adams et al., 1976; Rickett et al., 1986; Holstege et al., 1997). The mechanisms by which anticholinesterase agents interact with endogenous ACh systems in the brainstem and impair the control of breathing is poorly understood. In this study, we focused on the role of endogenous ACh transmission in modulating preBötC respiratory neuron excitability and in regulating respiratory pattern. We tested the hypothesis that there is cholinergic neurotransmission in the preBötC and XII nucleus; thus, inhibition of

acetylcholinesterases (AChEs) by physostigmine causes accumulation of ACh in the synaptic cleft and/or extracellular fluid that induces perturbations in respiratory rhythm and respiratory-related XIIn motor pattern similar to those induced by exogenously applied cholinergic agonists. Some of the results of this study have been presented in abstract form (Shao and Feldman, 2003).

EXPERIMENTAL PROCEDURES

Slice preparation

All animal use procedures were in accordance with The National Institutes of Health (USA) Guide for the Care and Use of Laboratory Animals and were approved by the UCLA Institutional Animal Care and Use committee. Efforts were made to minimize the number of animals used and their pain and suffering. Experiments were performed on a medullary slice preparation that retains functional respiratory networks and generates respiratory rhythm *in vitro* (Smith et al., 1991). Sprague–Dawley neonatal rat (0–3 days old) was anesthetized with isoflurane and then promptly decerebrated. The cerebellum was removed and the brainstem–spinal cord was isolated. The brainstem–spinal cord was mounted in the specimen vise of a Vibratome (VT 100; Technical Products International, Inc., MO, USA) oriented vertically with rostral end upward. The brainstem was sectioned serially in the coronal plane under a dissection microscope until the landmarks at the rostral boundary of the preBötC were visible. One transverse slice (500–650 μm thick) was cut. The slice was transferred to a recording chamber of 3-ml volume and stabilized with a threaded frame. The dissection and slicing were performed in an artificial cerebrospinal fluid (ACSF) bubbled with 95% O_2–5% CO_2 at room temperature. The ACSF contained (in mM) 128 NaCl, 3.0 KCl, 1.5 $CaCl_2$, 1.0 $MgSO_4$, 23.5 $NaHCO_3$, 0.5 NaH_2PO_4 and 30 glucose. During electrophysiological recording, the slice was continuously super-fused (2–3 ml min^{-1}) with ACSF with increased KCl (9 mM) that was recycled into a reservoir equilibrated with 95% O_2–5%CO_2. The ACSF in the recording chamber was maintained at 27±1 °C. All slices studied had rhythmic activity from XIIn that was similar in frequency and in temporal pattern to the respiratory activity recorded from en bloc brainstem–spinal cord preparations (Smith et al., 1991).

Electrophysiological recording

Neurons within 100 μm of the slice surface were visualized with an infrared-differential interference contrast microscope (Axioskop2; Carl Zeiss MicroImaging, Inc., Göttingen, Germany). The respiratory neurons we recorded fired in phase with the inspiratory bursts of XIIn rhythmic motor output and were located ventral to the nucleus ambiguus in the preBötC. To avoid confounding drug residue effects, only one inspiratory neuron was recorded from each preparation. Patch electrodes were pulled from thick wall (0.32 mm) borosilicate glass with tip size 1–1.5 μm (resistance: 4–6.5 MΩ). The electrode filling solution contained (in mM) 140 K-gluconate, 5.0 NaCl, 0.1 $CaCl_2$, 1.1 EGTA, 10 HEPES and 2.0 ATP (Mg^{2+} salt), pH adjusted to 7.3 with KOH. Intracellular signals were amplified and low pass-filtered at 2 kHz with a patch-clamp amplifier (MultiClamp 700A; Axon Instruments, Inc., CA, USA). A −10 mV junction potential was determined experimentally; reported values of potential are corrected values.

Respiratory-related rhythmic motor activity was recorded from the cut ends of XIIn with a suction electrode, amplified (×20,000) and band-pass filtered (1 Hz–3 kHz) with an amplifier (P5 series; Grass Instruments Co., MA, USA). Signals from intracellular recording and from XIIn were digitized at 10 kHz sampling frequency with DIGIDATA 1322A and software CLAMPEX 9 (Axon Instruments, Inc.) on a Pentium-based computer. The two channels of signals were saved as data files for further analyses off-line.

Drug application

Drugs were applied in two different ways: i) bath application, i.e. adding them to the perfusate. In this way, stable recordings from a respiratory neuron and from XIIn can be obtained and the drug concentrations for the slice are known and accurate (drugs take effect in 2–3 min after adding them to the perfusate in our perfusion system); ii) pressure microinjection into the preBötC or XII nucleus. In this way, the location of drug action can be precisely identified. We estimate 1:10 reduction on average in drug concentration from the injection pipette to the target region (Liu et al., 1990). For microinjection experiments, 5 μl calibrated glass pipette (Drummond Scientific Co. PA, USA) was pulled and the tip was broken to 6–9 μm diameter. The back of the pipette was connected to an air pressure source of 68–70 kPa. The pipette was mounted on a micromanipulator and advanced into the pre-BötC or XII nucleus, 100–200 μm below the slice surface. The injection volume was monitored by the displacement of the fluid meniscus using a microscope with a calibrated eyepiece reticule. A volume of 10 nl was injected which is estimated to diffuse to a region approximating the size of the preBötC within 10 s (Nicholson, 1985). When injecting into XII nucleus, 15 nl was injected. Drugs were dissolved in a pipette solution containing (in mM) 150 NaCl, 9 KCl, 1.5 $CaCl_2$, 1.0 $MgSO_4$, 10 HEPES and 30 glucose, pH adjusted to 7.4 with NaOH.

For bath application of cholinergic antagonists, the effects were measured 4–6 min after adding them. For bath application of physostigmine, since accumulation of endogenous ACh takes time if AChEs are inhibited, the effects were measured after 7–9 min. For microinjection of physostigmine, we measured the effects 1–2 min after injection. The recordings of the neuronal and XIIn activity immediately prior to drug application served as controls for each preparation.

(−)-Physostigmine sulfate, DH-β-E hydrobromide and 4-diphenylacetoxy-*N*-methylpiperidine methiodide (4-DAMP) were obtained from Sigma-Aldrich Co., MO, USA.

Data analysis

The respiratory-related motor activity recorded from XIIn was digitally integrated by full-wave rectification and low-pass-filtering at a time constant of 40 ms using a data analysis software package (DataView V4.1; W. J. Heitler, University of St. Andrews, UK). The intracellular signal was digitally low-pass-filtered at 1150 Hz except for measuring the phasic inward current of inspiratory neurons where the intracellular signal was filtered at 20 Hz. Respiratory periods were averaged from 10 consecutive periods in control or drug application conditions for each preparation and were used in statistical tests. Respiratory frequency was taken as reciprocal of period. The amplitude (and duration) of inspiratory

bursts of XIIn and the phasic inward current of inspiratory neurons were measured from the averaged envelope of five consecutive inspiratory periods triggered by the up-stroke of the integrated inspiratory XIIn bursts (DataView 4.1). Durations were measured at 20% of peak amplitude. Input resistance was measured using 30–50 pA 200 ms hyperpolarizing current pulses which caused 5–15 mV voltage step response in current-clamp mode. Then, they were averaged across neurons or preparations and presented as mean±S.D., except as indicated otherwise. *n*=Number of cells (for whole cell recording) or preparations (for XIIn motor output recording) is indicated. For experiments with application of physostigmine, paired *t*-tests were used taking the measurements before (pre-drug control) and during physostigmine application as a pair for each preparation to test the statistical significance of the response. For experiments with ACh antagonists, we measured electrophysiological parameters before and during application of antagonists and during physostigmine +antagonists for each neuron or each slice. One-way repeated measures ANOVA (Neter et al., 1990) was used to test the statistical significance for drug treatments. Post hoc comparison analyses based on Tukey were used to determine the significance of differences between antagonist application vs. control and between physostigmine+antagonists vs. antagonists. The procedure MIXED in the data analysis software package SAS (V8.2; SAS Institute Inc., NC, USA) was used for these analyses. In all analyses, $P \leq 0.05$ was the criterion for statistical significance.

Spontaneous excitatory postsynaptic current (sEPSC) data were analyzed with DataView 4.1. The program detected sEPSCs during expiratory periods by an optimally scaled-template recognition algorithm (Clements and Bekkers, 1997). Statistical significance for difference in rates, i.e. frequency of sEPSCs, was analyzed with a method detailed in Shao and Feldman (2001). Since the amplitude of sEPSCs is not normally distributed, statistical significance for difference in sEPSC amplitude distributions was analyzed with Kolmogorov-Smirnov test (Mini Analysis Program V5; Synaptosoft Co. GA, USA). Rates and amplitudes of sEPSCs were tested during application of cholinergic agents vs. control conditions for each neuron.

RESULTS

Differential effects of physostigmine injected into the preBötC and XII nucleus

To determine whether there is endogenous release of ACh in the preBötC that could affect breathing, we pressure microinjected physostigmine unilaterally into the preBötC in the medullary slice and recorded the respiratory-related motor activity from XIIn. Microinjection of physostigmine (150 μM, 10 nl) increased the frequency of rhythmic activity from control of 8.61±2.0 min^{-1} to 9.90±1.87 min^{-1} (116±13% of control, *n*=11; Fig. 1A, D). In addition, rhythmic activity became more regular (the variability of cycle-by-cycle periods decreased; Fig. 1B). These effects started within 30–40 s, gradually reached maximum at about 1–2 min following the injection; activity gradually recovered in the subsequent 10–20 min. These microinjections did not affect the amplitude (11.8±5.6 μV vs. control 11.9±6.0 μV) and duration (578±178 ms vs. control 589±194 ms) of integrated inspiratory bursts of XIIn motor output (Fig. 1E and F, *n*=10). The effects on frequency were the same following ipsilateral or contralateral injections.

Microinjection of physostigmine (150 μM, 15 nl) into the ipsilateral XII nucleus induced tonic activity (arrows in Fig. 1A trace four under "Physo"), increased the amplitude of integrated inspiratory bursts of XIIn from 11.1±5.0 μV to 13.2±5.3 μV (122±17% of control, *n*=9) and duration from 671±205 ms to 769±220 ms (117±22% of control; Fig. 1A, C, E, F) with no effect on frequency (7.85±2.19 min^{-1} vs. control of 7.89±2.42 min^{-1}; Fig. 1A, D). There was no effect when physostigmine was injected into the contralateral XII nucleus (Fig. 1A); this served as a control for injection into the preBötC and injection into the ipsilateral XII nucleus.

Effects of physostigmine on preBötC inspiratory neurons and respiratory-related XIIn rhythmic activity are similar to those of cholinergic agonists

PreBötC inspiratory neurons discharge in synchrony with the inspiratory burst activity of XIIn motor output; a subset of these neurons are hypothesized to generate respiratory rhythm (Gray et al., 1999; Feldman et al., 2003). To determine the cellular mechanisms underlying the effects of inhibition of AChEs on respiratory pattern, we patch-clamped preBötC inspiratory neurons and simultaneously recorded respiratory-related rhythmic motor output from XIIn. Bath application of physostigmine (10 μM) induced tonic activity, increased respiratory frequency from 8.25±1.93 min^{-1} to 12.45±2.98 min^{-1} (152±20% of control, *n*=11), increased the amplitude from 12.0±8.3 μV to 13.7±8.4 μV (122±25% of control, *n*=12) and duration from 498±118 ms to 664±119 ms (136±20% of control) of integrated inspiratory bursts of XIIn motor output (Fig. 3A, B, D). These effects on the motor nerve output are consistent with the actions of physostigmine on both the pre-BötC and XII nucleus. Bath application of physostigmine depolarized preBötC inspiratory neurons (Fig. 2A, B). In neurons voltage-clamped at −65 mV, physostigmine: i) induced a tonic inward current of 6.3±10.6 pA (*n*=6, Fig. 3A) measured during expiratory periods; ii) increased the whole-cell membrane noise; iii) decreased the amplitude of inspiratory drive currents from control of 83.4±58.2 pA to 62.8±40.8 pA (79±16% of control, *n*=12) without any consistent effect on the duration (605±111 ms vs. control of 572±154 ms; Fig. 3A, B, D), and; iv) increased the frequency of sEPSCs during expiratory periods from 3.42±2.85 s^{-1} to 4.46±3.32 s^{-1} (163±103% of control, *n*=10) without significant change in the amplitude (control: −23.9±12.3 pA; physostigmine: −23.5±13.3 pA). Statistical analysis for each neuron, with the assumption that each series of sEPSCs was a Poisson process (see Experimental Procedures), showed that the increase in frequency was statistically significant in six of 10 neurons; the frequency did not change in two neurons and decreased in two neurons. Bath application of physostigmine also decreased the input resistance from 293.1±139.8 MΩ to 202.2±99.3 MΩ (73±22% of control) without affecting the threshold for action potential generation (control: −54.1±1.5 mV; physostigmine: −55.0±2.7 mV), suggesting an enhancement of excitability in these neurons. These effects of physostigmine are similar to that of bath application of the cholinergic agonists muscarine and nicotine (Shao and Feldman, 2000, 2001), except the responses started and reached their maxima slower in physostigmine experiments. These effects appeared at 4–6 min and reached their maxima at 5–7 min following addition of physostigmine into the perfusate (Fig. 2). These responses slightly desensitized in the continuous presence of physostigmine.

Effects of AChR antagonists and their actions on physostigmine induced-responses

In the presence of tetrodotoxin (TTX), the inward current induced by exogenously applied ACh on preBötC inspiratory neurons can be blocked by 4-DAMP (Shao and Feldman, 2000). The effects of low concentrations of nicotine on preBötC inspiratory neurons and on the pattern of respiratory-related motor activity can be blocked by DH-β-E (Shao and Feldman, 2002). We tested whether these antagonists can block the effects of endogenously released ACh when AChEs are inhibited.

Bath application of 4-DAMP (2 μM) did not affect the frequency, amplitude or duration of integrated inspiratory bursts of XIIn motor output (*n*=6, Table 1). Subsequent application of physostigmine (10 μM) increased respiratory frequency to 123±19% of control (*n*=5) without consistent changes in amplitude and duration (Table 1, Fig. 4B, C).

Bath application of 4-DAMP increased the input resistance to 116±9% of control without affecting the action potential threshold of preBötC inspiratory neurons. In voltage-clamp mode, 4-DAMP did not alter the amplitude and duration of phasic inspiratory drive currents (*n*=7, Fig. 4A, B). There was no significant change in the frequency and amplitude of sEPSCs (Table 1, Fig. 4C). Subsequent addition of physostigmine in the presence of 4-DAMP had no significant effect on the amplitude and duration of inspiratory drive currents, input resistance, action potential threshold, or the frequency and amplitude of sEPSCs (*n*=5, Table 1, Fig. 4A–C).

Bath application of DH-β-E (0.2 μM) had no significant effect on the frequency (*n*=9), amplitude or duration of integrated inspiratory bursts of XIIn motor output (Table 2). Subsequent addition of physostigmine (10 μM) increased the amplitude of integrated inspiratory bursts of XIIn to 116±25% of control (*n*=7) without consistent effects on respiratory frequency and duration (Table 2, Fig. 5A–C).

Bath application of DH-β-E did not alter the amplitude and duration of phasic inspiratory drive currents (*n*=7, Fig. 5A, B), nor did it significantly affect the input resistance, action potential threshold, the frequency and amplitude of sEPSCs (Table 2, Fig. 5C). Subsequent addition of physostigmine in the presence of DH-β-E had no significant effect on cellular parameters such as the amplitude and duration of inspiratory drive currents, the input resistance, action potential threshold, or the frequency and amplitude of sEPSCs (*n*=7, Table 2, Fig. 5A–C).

Concurrent bath application of 4-DAMP (2 μM) and DH-β-E (0.2 μM) had no significant effect on the frequency (*n*=7), amplitude, or duration of integrated inspiratory bursts of XIIn motor output (Table 3). Subsequent addition of physostigmine (10 μM) decreased respiratory frequency to 84±8% and decreased the amplitude of integrated inspiratory bursts of XIIn to 85±13% of pre-physostigmine levels (*n*=7) without any significant change in duration (Table 3, Fig. 6A–C).

Concurrent bath application 4-DAMP and DH-β-E did not alter the amplitude and duration of phasic inspiratory drive currents (*n*=7, Table 3), input resistance, action potential threshold or the frequency and amplitude of sEP-SCs (Table 3, Fig. 6A–C) in preBötC

inspiratory neurons. Subsequent addition of physostigmine had no effect on the amplitude and duration of inspiratory drive currents, sEPSC frequency and amplitude, input resistance, or action potential threshold (Table 3, Fig. 6A–C).

DISCUSSION

Microinjection of the anticholinesterase drug physostigmine into the preBötC increased the frequency of respiratory-related rhythmic motor nerve activity. Injection into XII nucleus induced tonic activity, increased the amplitude and duration of the integrated inspiratory bursts of XIIn, but did not alter the burst frequency. These observations are consistent with the hypothesis that the preBötC is an essential site for respiratory rhythm generation (Smith et al., 1991). These results suggest that there is cholinergic neurotransmission in the preBötC and that physiologically relevant levels of ACh release play a role in the regulation of respiratory frequency. Our data also suggest that cholinergic neurotransmission in XII nucleus modulates the amplitude and duration of inspiratory burst activity, and the tonic activity of XIIn motor output. In patch-clamped preBötC inspiratory neurons, physostigmine induced a tonic inward current, increased the membrane noise, decreased the amplitude of phasic inspiratory drive current, increased the frequency of sEPSCs, and decreased whole cell input resistance without affecting the threshold for action potential generation. In addition, bath application of 4-DAMP, which blocks mAChRs, increased the input resistance. The effects induced by physostigmine at both the cellular and systems levels are similar to the responses induced by exogenously applied cholinergic agonists (Shao and Feldman, 2000, 2001), except for a longer time delay in onset. These results are consistent with the hypothesis that inhibition of AChEs elevates ACh levels in the synaptic cleft and/or extracellular fluid in the preBötC and XII nucleus due to accumulation of endogenously released ACh. Furthermore, these results suggest the modulation of the excitability of inspiratory neurons and of excitatory neurotransmission in the preBötC by endogenous ACh could underlie cholinergic regulation of respiratory frequency. The frequency effect of bath-applied physostigmine was partially blocked by 4-DAMP and completely blocked by DH-β-E, while the amplitude effect of physostigmine was partially blocked by DH-β-E and completely blocked by 4-DAMP. In the presence of both 4-DAMP and DH-β-E, physostigmine induced opposite effects on respiratory frequency and on the amplitude of integrated inspiratory bursts of XIIn motor output. These results suggest that both mAChRs, which are sensitive to 4-DAMP, and nAChRs, which are sensitive to DH-β-E, mediate the effects of endogenous ACh on preBötC neuronal function and on respiratory pattern. These results do not exclude the possibility that endogenous ACh also acts on other nAChRs insensitive to DH-β-E.

In addition to its anticholinesterase action, physostigmine has direct effects on nAChRs. At low concentrations (1–10 μM), physostigmine acts as a nicotinic allosteric potentiating ligand on certain subtypes of nAChRs (Pereira et al., 2002). Low concentrations (≤10 μM) of physostigmine potentiate ionic currents induced by low concentrations of ACh but inhibit ionic currents induced by high concentrations of ACh (Zwart et al., 2000). The effects of physostigmine on preBötC inspiratory neurons and respiratory-related motor pattern we observed in this study are unlikely to be solely due to the direct actions of physostigmine on nAChRs because the effects of microinjection of physostigmine take 30–40 s to manifest

and of bath application take >4 min to manifest (consistent with the time needed for accumulation of ACh). Under our experimental conditions, we would expect that any direct effects on AChRs would appear within seconds for microinjection and within 2–3 min for bath application (Shao and Feldman, 2001). Our study does not rule out the possibility that, in addition to its anticholinesterase actions, direct actions of physostigmine on ACh receptors may play a role in the physostigmine effects on inspiratory neurons and respiratory pattern.

The roles of mAChRs and nAChRs in endogenous cholinergic regulation of respiratory pattern

Physostigmine reduced the input resistance of preBötC inspiratory neurons. This could be due to opening of post-/ extra-synaptic ACh channels and/or indirectly enhancing excitatory neurotransmission by ACh. Our previous study showed that there are 4-DAMP-sensitive mAChRs in pre-BötC inspiratory neurons; in the presence of TTX, local application of ACh on preBötC inspiratory neurons induces an inward current associated with reduction of input resistance which can be blocked by 4-DAMP (Shao and Feldman, 2000). In this study, 4-DAMP alone increased the input resistance of preBötC inspiratory neurons. These data suggest that 4-DAMP-sensitive mAChRs on preBötC inspiratory neurons are targets of endogenous ACh and activation of these receptors modulates the excitability of these neurons.

In addition, 4-DAMP blocked the effects induced by physostigmine except it reduced, but did not completely abolish the physostigmine effects on respiratory frequency. These results are consistent with the observations of Murakoshi et al. (1985) that the frequency increase induced by exogenously applied ACh in the brainstem–spinal cord preparation can be greatly reduced, but is not completely abolished by atropine, whereas it can be completely abolished by a combination of atropine and DH-β-E. Our data suggest that endogenous ACh modulates the excitability of preBötC inspiratory neurons via M3-like mAChRs on these neurons; this may be one of the mechanisms underlying cholinergic regulation of respiratory frequency.

In the presence of DH-β-E, physostigmine altered neither neuronal parameters nor the frequency of respiratory-related motor activity. These results appear counterintuitive, since when nAChRs are blocked by DH-β-E, elevated levels of ACh by physostigmine could activate mAChRs that should induce effects similar to application of mAChR agonists. There are two possible interpretations: i) physostigmine may have direct effects on DH-β-E-insensitive nAChRs that counteract the ACh actions on mAChRs. Physostigmine acts as a nicotinic allosteric potentiating ligand on α4β2 nAChRs (Pereira et al., 2002). At concentrations of 10 μM, physostigmine potentiates or depresses ACh-induced activation of α4β2 and α4β4 nAChRs depending on ACh concentration (Zwart et al., 2000). We consider this an unlikely interpretation for our results, because α4β2 and α4β4 nAChRs would not be activated in the presence of DH-β-E; ii) ACh potentiates inhibitory GABAergic and/or glycinergic neurotransmission via DH-β-E-insensitive receptors. Endogenous ACh, via DH-β-E-sensitive nAChRs, enhances GABAergic and glycinergic synaptic transmission to cardiac vagal neurons in the nucleus ambiguus (Wang et al., 2003). Activation of nAChRs

enhances GABAergic transmission in the dorsal motor nucleus of the vagus and in the hippocampus (Bertolino et al., 1997; Alkondon et al., 2000; Alkondon and Albuquerque, 2001). We speculate that the frequency effects of ACh via DH-β-E-sensitive nAChRs are dominant under control conditions. In the presence of DH-β-E, however, the nicotinic potentiation of GABAergic and/or glycinergic transmission via DH-β-E-insensitive nAChRs counteracts the excitatory effects of activation of mAChRs by ACh. Such inhibitory effects were unmasked when mAChRs were blocked in the conditions of co-application of DH-β-E and 4-DAMP, resulting in a significant decrease in respiratory frequency observed in the present study (Fig. 6; Table 3). Monteau et al. (1990) reported that mecamylamine does not block the frequency effects of exogenously applied ACh in the brainstem–spinal cord preparation. The inconsistency between these results and our data are probably due to the non-specific nature of mecamylamine as a nicotinic antagonist (Papke et al., 2001). Mecamylamine also acts on DH-β-E-insensitive nAChRs; therefore, the inhibitory effects of these nAChRs which counteract the effects of activation of mAChRs are abolished. This interpretation may also account for the observation that DH-β-E at higher concentrations (5 μM), which may have non-specific effects on other nAChRs (we have shown that DH-β-E at concentration of 0.2 μM completely blocks the effects of nicotine application on inspiratory neurons and on respiratory pattern in slice preparations; Shao and Feldman, 2001), does not reduce the frequency effects of exogenously applied ACh in the brainstem–spinal cord preparation (Murakoshi et al., 1985). Differences in action sites (synaptic vs. extrasynaptic) and action kinetics for endogenously released ACh following inhibition of AChEs compared with exogenously applied ACh without inhibition of AChEs, as well as differences between preparations (slice vs. en bloc brainstem–spinal cord) may also contribute to the discrepancies between our data and the results of Murakoshi et al. (1985) and of Monteau et al. (1990). Consistent with the idea that endogenous ACh potentiates inhibitory GABAergic and/or glycinergic transmission via DH-β-E-insensitive nAChRs, we observed that physostigmine in the presence of DH-β-E and 4-DAMP decreased the amplitude of integrated inspiratory bursts of XIIn motor output (Fig. 6; Table 3).

In the presence of DH-β-E, physostigmine increased the amplitude of integrated inspiratory bursts of XIIn (Fig. 5B, C) while 4-DAMP alone completely blocked the amplitude effects of physostigmine. These data suggest that, in XII motoneurons, ACh effects via mAChRs are dominant compared with those via nAChRs.

Source of cholinergic projection

Cholinergic neurons in the pedunculopontine tegmentum and the laterodorsal pontine tegmentum (PPT/LDT), one of the two main cholinergic projection systems in the brain, have descending projections to the medullary reticular nuclei and the lateral reticular nucleus (Woolf and Butcher, 1989; Jones, 1990; Woolf, 1991), and probably also to the preBötC and XII nucleus. If this is the case, although our slice preparation does not contain the PTT/LDT, the remaining axons or terminals can still release ACh in the preBötC and XII nucleus as synaptic terminals and boutons can release neurotransmitters after they are isolated from cell bodies (Haage et al., 1998; Akaike and Moor-house, 2003). ACh may also be released from cholinergic neurons present locally in the rostral ventrolateral medulla (Jones, 1990; Ruggiero et al., 1990).

Synaptic/volume transmission and pre-or post-synaptic modulation

Since cholinergic EPSCs have not been observed in pre-BötC neurons and since the phasic inspiratory drive current as well as sEPSCs recorded from preBötC inspiratory neurons can be completely abolished by CNQX (Shao and Feldman, 2001), the effects of endogenous ACh are probably modulatory through pre-, post- and/or extra-synaptic mechanisms. We have determined that activation of M3-like mAChRs at post- and/or extra-synaptic sites of pre-BötC inspiratory neurons modulates their excitability and regulates respiratory-related motor activity from XIIn (Shao and Feldman, 2000). Endogenously released ACh may also act on other mAChR subtypes pre-synaptically and contribute to modulation of synaptic transmission onto pre-BötC neurons. In addition to classic synaptic transmission mechanisms, cholinergic modulation of respiratory frequency and pattern in the preBötC and XII nucleus may act via mechanisms of volume transmission (Zoli et al., 1999). Cholinergic synaptic mechanisms such as pre-, post-, extra-synaptic, pre-terminal and/or volume transmission underlying respiratory regulation in the preBötC remain to be elucidated.

Cholinergic transmission in XII nucleus

Although this investigation primarily focused on endogenous cholinergic neurotransmission in the preBötC, by microinjection of physostigmine into XII nucleus, we found that endogenous ACh release in the preBötC and in XII nucleus play differential roles in respiratory regulation. The cholinergic mechanisms in XII nucleus have their own physiological and pathological significance. Reduction of tonic and phasic activity of upper airway dilatory muscles during sleep can result in airway collapse leading to obstructive sleep apnea (Remmers et al., 1978; Horner et al., 2002). XII nuclei innervate tongue muscles (Aldes, 1995; Dobbins and Feldman, 1995) and play an important role in maintaining upper airway patency (Fuller et al., 1999). XII nuclei receive cholinergic inputs. The terminals which make synaptic contact with XII motoneurons contain both AChEs and choline acetyltransferase (Lewis and Shute, 1966; Connaughton et al., 1986; Arvidsson et al., 1997) that provide anatomical substrates for the electrophysiological findings in this study. The origin of these cholinergic terminals is probably the PPT/LDT (Woolf and Butcher, 1989), while medullary cholinergic neurons, e.g. neurons in medial reticular formation and lateral reticular nucleus, may also contribute (Lauterborn et al., 1993; Holmes et al., 1994). nAChRs are present on XII motoneurons and activation of nAChRs excites these neurons (Chamberlin et al., 2002; Robinson et al., 2002). Activation of presynaptic M2 mAChRs modulates excitatory amino-acid transmission onto XII motoneurons (Bellingham and Berger, 1996). In this study, we show that there is endogenous ACh release within XII nucleus that enhances the tonic activity and the amplitude and duration of inspiratory bursts of XIIn motor output. The endogenous ACh probably modulates the excitability of XII motoneurons via nAChRs and mAChRs. This may be an important mechanism underlying the clinical therapeutic effects of physostigmine on sleep apnea (Hedner et al., 2003).

Organophosphorus compounds, including nerve agents, are inhibitors of AChE; central respiratory arrest is a contributory cause of death during acute organophosphate intoxication (Adams et al., 1976; Rickett et al., 1986; Holstege et al., 1997). Unlike the peripheral cholinergic mechanisms, the central mechanisms underlying respiratory failure caused by

organophosphates are poorly understood. Since endogenously released ACh in the preBötC and in XII nucleus plays different functional roles in modulation of respiratory frequency and pattern as shown in this study, we postulate that accumulation of ACh in the preBötC, XII nucleus and probably other respiratory motoneuron groups, e.g. the phrenic nucleus, contributes differentially to respiratory arrest during acute organophosphate poisoning.

Acknowledgments

This work was supported by Tobacco-Related Disease Research Program (California) grant 10RT-0241 and NIH grant HL40959.

Abbreviations

ACh	acetylcholine
AChEs	acetylcholinesterases
ACSF	artificial cerebrospinal fluid
DH-β-E	dihydro-β-erythroidine
LDT	laterodorsal pontine tegmentum
mAChR	muscarinic acetylcholine receptor
nAChR	nicotinic acetylcholine receptor
PPT	pedunculopontine tegmentum
preBötC	preBötzinger complex
sEPSC	spontaneous excitatory postsynaptic current
TTX	tetrodotoxin
XII nucleus	the hypoglossal nucleus
XIIn	the hypoglossal nerve roots
4-DAMP	4-diphenylacetoxy-*N*-methylpiperidine methiodide

References

Adams GK, Yamamura HI, O'Leary JF. Recovery of central respiratory function following anticholinesterase intoxication. Eur J Pharmacol. 1976; 38:101–112. [PubMed: 954819]

Akaike N, Moorhouse AJ. Techniques: applications of the nerve-bouton preparation in neuropharmacology. Trends Pharmacol Sci. 2003; 24:44–47. [PubMed: 12498731]

Aldes LD. Subcompartmental organization of the ventral (protrusor) compartment in the hypoglossal nucleus of the rat. J Comp Neurol. 1995; 353:89–108. [PubMed: 7714251]

Alkondon M, Albuquerque EX. Nicotinic acetylcholine receptor alpha7 and alpha4beta2 subtypes differentially control GABAergic input to CA1 neurons in rat hippocampus. J Neurophysiol. 2001; 86:3043–3055. [PubMed: 11731559]

Alkondon M, Braga MF, Pereira EF, Maelicke A, Albuquerque EX. alpha7 nicotinic acetylcholine receptors and modulation of gabaergic synaptic transmission in the hippocampus. Eur J Pharmacol. 2000; 393:59–67. [PubMed: 10770998]

Arvidsson U, Riedl M, Elde R, Meister B. Vesicular acetylcholine transporter (VAChT) protein: a novel and unique marker for cholinergic neurons in the central and peripheral nervous systems. J Comp Neurol. 1997; 378:454–467. [PubMed: 9034903]

Bellingham MC, Berger AJ. Presynaptic depression of excitatory synaptic inputs to rat hypoglossal motoneurons by muscarinic M2 receptors. J Neurophysiol. 1996; 76:3758–3770. [PubMed: 8985874]

Bellingham MC, Ireland MF. Contribution of cholinergic systems to state-dependent modulation of respiratory control. Respir Physiol Neurobiol. 2002; 131:135–144. [PubMed: 12107001]

Bertolino M, Kellar KJ, Vicini S, Gillis RA. Nicotinic receptor mediates spontaneous GABA release in the rat dorsal motor nucleus of the vagus. Neuroscience. 1997; 79:671–681. [PubMed: 9219932]

Burton MD, Nouri K, Baichoo S, Samuels-Toyloy N, Kazemi H. Ventilatory output and acetylcholine: perturbations in release and muscarinic receptor activation. J Appl Physiol. 1994; 77:2275–2284. [PubMed: 7868445]

Chamberlin NL, Bocchiaro CM, Greene RW, Feldman JL. Nicotinic excitation of rat hypoglossal motoneurons. Neuroscience. 2002; 115:861–870. [PubMed: 12435424]

Clements JD, Bekkers JM. Detection of spontaneous synaptic events with an optimally scaled template. Biophys J. 1997; 73:220–229. [PubMed: 9199786]

Connaughton M, Priestley JV, Sofroniew MV, Eckenstein F, Cuello AC. Inputs to motoneurones in the hypoglossal nucleus of the rat: light and electron microscopic immunocytochemistry for choline acetyltransferase, substance P and enkephalins using monoclonal antibodies. Neuroscience. 1986; 17:205–224. [PubMed: 2421199]

Dehkordi O, Haxhiu MA, Millis RM, Dennis GC, Kc P, Jafri A, Khajavi M, Trouth CO, Zaidi SI. Expression of alpha-7 nAChRs on spinal cord-brainstem neurons controlling inspiratory drive to the diaphragm. Respir Physiol Neurobiol. 2004; 141:21–34. [PubMed: 15234673]

Dobbins EG, Feldman JL. Differential innervation of protruder and retractor muscles of the tongue in rat. J Comp Neurol. 1995; 357:376–394. [PubMed: 7673474]

Dominguez del Toro E, Juiz JM, Peng X, Lindstrom J, Criado M. Immunocytochemical localization of the alpha 7 subunit of the nicotinic acetylcholine receptor in the rat central nervous system. J Comp Neurol. 1994; 349:325–342. [PubMed: 7852628]

Feldman JL, Mitchell GS, Nattie EE. Breathing: rhythmicity, plasticity, chemosensitivity. Annu Rev Neurosci. 2003; 26:239–266. [PubMed: 12598679]

Fuller DD, Williams JS, Janssen PL, Fregosi RF. Effect of co-activation of tongue protrudor and retractor muscles on tongue movements and pharyngeal airflow mechanics in the rat. J Physiol. 1999; 519(Pt 2):601–613. [PubMed: 10457075]

Gilman S, Chervin RD, Koeppe RA, Consens FB, Little R, An H, Junck L, Heumann M. Obstructive sleep apnea is related to a thalamic cholinergic deficit in MSA. Neurology. 2003; 61:35–39. [PubMed: 12847153]

Gray PA, Rekling JC, Bocchiaro CM, Feldman JL. Modulation of respiratory frequency by peptidergic input to rhythmogenic neurons in the preBötzinger complex. Science. 1999; 286:1566–1568. [PubMed: 10567264]

Haage D, Karlsson U, Johansson S. Heterogeneous presynaptic Ca^{2+}channel types triggering GABA release onto medial pre-optic neurons from rat. J Physiol. 1998; 507(Pt 1):77–91. [PubMed: 9490820]

Hedner J, Kraiczi H, Peker Y, Murphy P. Reduction of sleep-disordered breathing after physostigmine. Am J Respir Crit Care Med. 2003; 168:1246–1251. [PubMed: 12958052]

Holmes CJ, Mainville LS, Jones BE. Distribution of cholinergic, GABAergic and serotonergic neurons in the medial medullary reticular formation and their projections studied by cytotoxic lesions in the cat. Neuroscience. 1994; 62:1155–1178. [PubMed: 7845592]

Holstege CP, Kirk M, Sidell FR. Chemical warfare: nerve agent poisoning. Crit Care Clin. 1997; 13:923–942. [PubMed: 9330846]

Horner RL, Liu X, Gill H, Nolan P, Liu H, Sood S. Effects of sleep-wake state on the genioglossus vs. diaphragm muscle reponse to $CO_{(2)}$ in rats. J Appl Physiol. 2002; 92:878–887. [PubMed: 11796705]

Jones BE. Immunohistochemical study of choline acetyltransferase-immunoreactive processes and cells innervating the pontomedullary reticular formation in the rat. J Comp Neurol. 1990; 295:485–514. [PubMed: 2351765]

Kinney HC, Filliano JJ, Sleeper LA, Mandell F, Valdes-Dapena M, White WF. Decreased muscarinic receptor binding in the arcuate nucleus in sudden infant death syndrome. Science. 1995; 269:1446–1450. [PubMed: 7660131]

Lauterborn JC, Isackson PJ, Montalvo R, Gall CM. In situ hybridization localization of choline acetyltransferase mRNA in adult rat brain and spinal cord. Brain Res Mol Brain Res. 1993; 17:59–69. [PubMed: 8381910]

Levey AI, Kitt CA, Simonds WF, Price DL, Brann MR. Identification and localization of muscarinic acetylcholine receptor proteins in brain with subtype-specific antibodies. J Neurosci. 1991; 11:3218–3226. [PubMed: 1941081]

Lewis PR, Shute CC. The distribution of cholinesterase in cholinergic neurons demonstrated with the electron microscope. J Cell Sci. 1966; 1:381–390. [PubMed: 5968988]

Liu G, Feldman JL, Smith JC. Excitatory amino acid-mediated transmission of inspiratory drive to phrenic motoneurons. J Neurophysiol. 1990; 64:423–436. [PubMed: 1976765]

Lydic R, Baghdoyan HA. Pedunculopontine stimulation alters respiration and increases ACh release in the pontine reticular formation. Am J Physiol. 1993; 264:R544–554. [PubMed: 8457006]

Mallard C, Tolcos M, Leditschke J, Campbell P, Rees S. Reduction in choline acetyltransferase immunoreactivity but not muscarinic-m2 receptor immunoreactivity in the brainstem of SIDS. J Neuropathol Exp Neurol. 1999; 58:255–264. [PubMed: 10197817]

Mallios VJ, Lydic R, Baghdoyan HA. Muscarinic receptor subtypes are differentially distributed across brain stem respiratory nuclei. Am J Physiol. 1995; 268:L941–L949. [PubMed: 7611435]

Monteau R, Morin D, Hilaire G. Acetylcholine and central chemosensitivity: in vitro study in the newborn rat. Respir Physiol. 1990; 81:241–253. [PubMed: 2263784]

Murakoshi T, Suzue T, Tamai S. A pharmacological study on respiratory rhythm in the isolated brainstem-spinal cord preparation of the newborn rat. Br J Pharmacol. 1985; 86:95–104. [PubMed: 2413943]

Nattie EE, Li A. Ventral medulla sites of muscarinic receptor subtypes involved in cardiorespiratory control. J Appl Physiol. 1990; 69:33–41. [PubMed: 2118496]

Neter, J.; Wasserman, W.; Kutner, MH. Applied linear statistical models. Homewood, IL: Richard D Irwin, Inc; 1990. Repeated measures and related designs; p. 1035-1073.

Nicholson C. Diffusion from an injected volume of a substance in brain tissue with arbitrary volume fraction and tortuosity. Brain Res. 1985; 333:325–329. [PubMed: 3995298]

Papke RL, Sanberg PR, Shytle RD. Analysis of mecamylamine stereoisomers on human nicotinic receptor subtypes. J Pharmacol Exp Ther. 2001; 297:646–656. [PubMed: 11303054]

Pereira EF, Hilmas C, Santos MD, Alkondon M, Maelicke A, Albuquerque EX. Unconventional ligands and modulators of nicotinic receptors. J Neurobiol. 2002; 53:479–500. [PubMed: 12436414]

Remmers JE, deGroot WJ, Sauerland EK, Anch AM. Pathogenesis of upper airway occlusion during sleep. J Appl Physiol. 1978; 44:931–938. [PubMed: 670014]

Rickett DL, Glenn JF, Beers ET. Central respiratory effects versus neuromuscular actions of nerve agents. Neurotoxicology. 1986; 7:225–236. [PubMed: 3714123]

Robinson DM, Peebles KC, Kwok H, Adams BM, Clarke LL, Woollard GA, Funk GD. Prenatal nicotine exposure increases apnoea and reduces nicotinic potentiation of hypoglossal inspiratory output in mice. J Physiol. 2002; 538:957–973. [PubMed: 11826179]

Ruggiero DA, Giuliano R, Anwar M, Stornetta R, Reis DJ. Anatomical substrates of cholinergic-autonomic regulation in the rat. J Comp Neurol. 1990; 292:1–53. [PubMed: 2312784]

Shao XM, Feldman JL. Acetylcholine modulates respiratory pattern: effects mediated by M3-like receptors in preBötzinger complex inspiratory neurons. J Neurophysiol. 2000; 83:1243–1252. [PubMed: 10712452]

Shao XM, Feldman JL. Mechanisms underlying regulation of respiratory pattern by nicotine in preBötzinger complex. J Neurophysiol. 2001; 85:2461–2467. [PubMed: 11387392]

Shao XM, Feldman JL. Pharmacology of nicotinic receptors in preBotzinger complex that mediate modulation of respiratory pattern. J Neurophysiol. 2002; 88:1851–1858. [PubMed: 12364511]

Shao XM, Feldman JL. Endogenous cholinergic neurotransmission in preBötzinger complex modulates excitability of inspiratory neurons and regulates respiratory pattern. Soc Neurosci. 2003:Abstr 247.5.

Smith JC, Ellenberger HH, Ballanyi K, Richter DW, Feldman JL. Pre-Bötzinger complex: a brainstem region that may generate respiratory rhythm in mammals. Science. 1991; 254:726–729. [PubMed: 1683005]

Smith JC, Feldman JL. In vitro brainstem-spinal cord preparations for study of motor systems for mammalian respiration and locomotion. J Neurosci Methods. 1987; 21:321–333. [PubMed: 2890797]

Wada E, Wada K, Boulter J, Deneris E, Heinemann S, Patrick J, Swanson LW. Distribution of alpha 2, alpha 3, alpha 4, and beta 2 neuronal nicotinic receptor subunit mRNAs in the central nervous system: a hybridization histochemical study in the rat. J Comp Neurol. 1989; 284:314–335. [PubMed: 2754038]

Wang J, Wang X, Irnaten M, Venkatesan P, Evans C, Baxi S, Mendelowitz D. Endogenous acetylcholine and nicotine activation enhances GABAergic and glycinergic inputs to cardiac vagal neurons. J Neurophysiol. 2003; 89:2473–2481. [PubMed: 12611951]

Weinstock M, Roll D, Zilberman Y. An analysis of the respiratory stimulant effect of physostigmine and neostigmine in the conscious rabbit. Clin Exp Pharmacol Physiol. 1981; 8:151–158. [PubMed: 6788414]

Woolf NJ. Cholinergic systems in mammalian brain and spinal cord. Prog Neurobiol. 1991; 37:475–524. [PubMed: 1763188]

Woolf NJ, Butcher LL. Cholinergic systems in the rat brain: IV. Descending projections of the pontomesencephalic tegmentum. Brain Res Bull. 1989; 23:519–540. [PubMed: 2611694]

Zoli M, Jansson A, Sykova E, Agnati LF, Fuxe K. Volume transmission in the CNS and its relevance for neuropsychopharmacology. Trends Pharmacol Sci. 1999; 20:142–150. [PubMed: 10322499]

Zwart R, van Kleef RG, Gotti C, Smulders CJ, Vijverberg HP. Competitive potentiation of acetylcholine effects on neuronal nicotinic receptors by acetylcholinesterase-inhibiting drugs. J Neurochem. 2000; 75:2492–2500. [PubMed: 11080202]

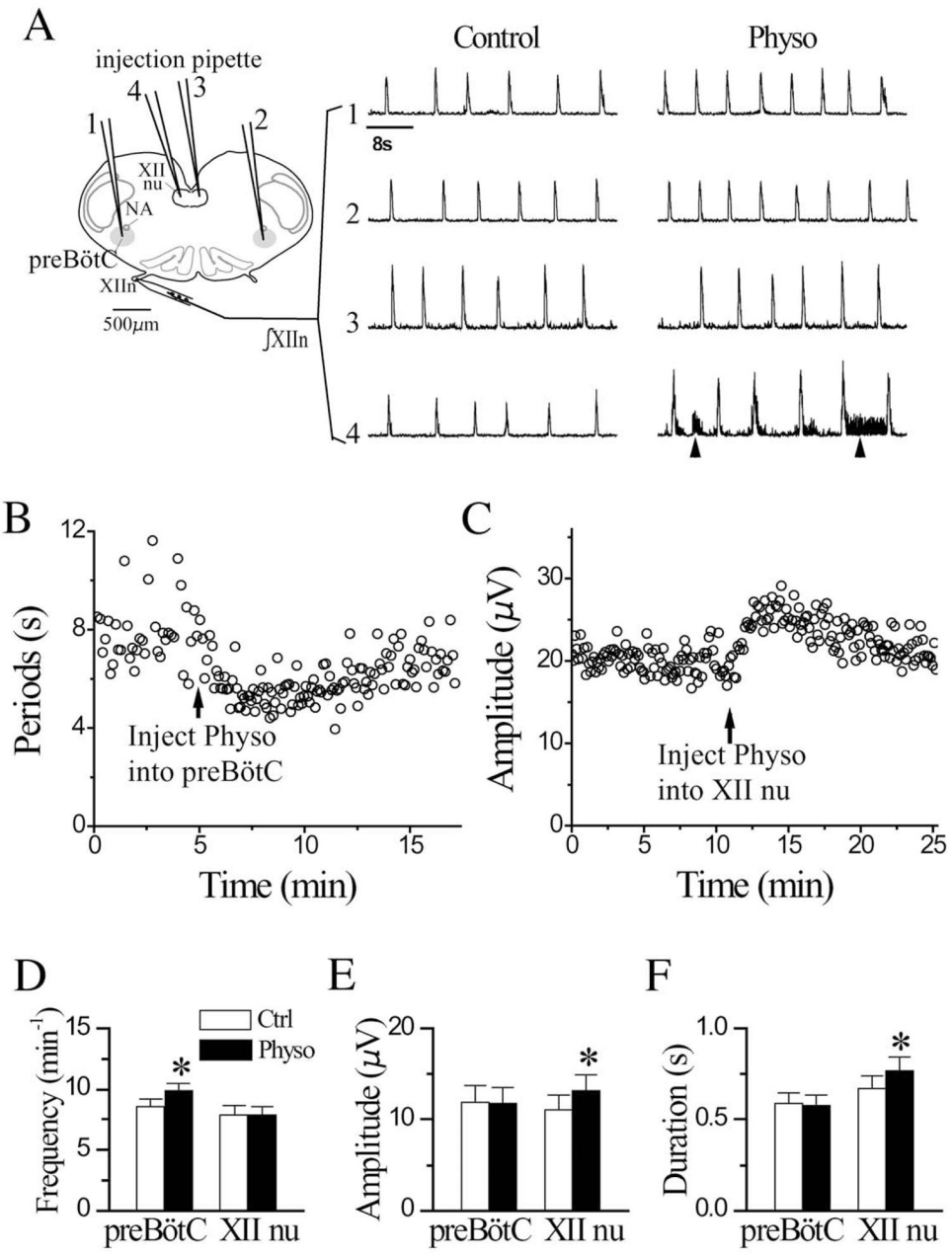

Fig. 1.

Pressure microinjection of Physo (150 μM, 10 nl) into the preBötC increased frequency of integrated rhythmic activity of hypoglossal nerve (∫XIIn) while injection into XII nu induced tonic activity, increased amplitude and duration of integrated inspiratory bursts of XIIn. (A) Traces 1–4 indicate injections into the ipsilateral preBötC (1), contralateral preBötC (2), contralateral XII nu (3) and ipsilateral XII nu (4). The injection pipettes were inserted 100–200 μm below the surface of the slice. “Control” traces were prior to, and “Physo” traces were at least 1 min after Physo injection. Arrowheads on trace 4 indicate tonic activity. Traces 1, 2, 3 and 4 were from different preparations. (B) Physo injection into the preBötC decreased respiratory cycle periods and variability of the periods. Arrow

indicates the time of injection. The data were from the same preparation as trace 2 in panel A. (C) Physo injection into ipsilateral XII nu increased the amplitude of integrated inspiratory bursts of XIIn. Arrow indicates the time of injection. Summaries of the Physo effects on respiratory frequency (D), amplitude (E) and duration (F) of integrated inspiratory bursts of XIIn (mean±S.E.). Respiratory frequency was determined as the reciprocal of the average of 10 consecutive respiratory periods for each condition. The amplitude and duration were determined with averaged envelope of five consecutive inspiratory bursts for each condition. * Statistical significance of Physo injection vs. control condition (paired *t*-test). Numbers of preparations (*n*) for every experiment are indicated in the text of Results section.

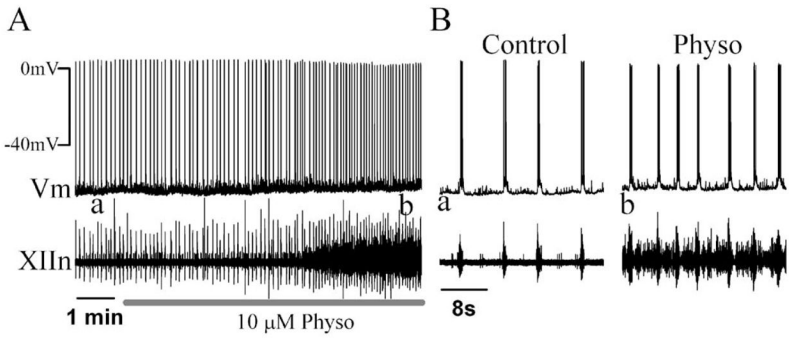

Fig. 2.

(A) Bath application of Physo (10 μM) depolarized preBötC inspiratory neurons in current-clamp mode. (B) Effects of Physo on an extended time scale; a and b correspond to the labeled times a and b in panel A.

Amp, amplitude of integrated inspiratory bursts; Anta, 4-DAMP+DH-β-E; Ctrl, control; Frq, respiratory frequency; Im, membrane current; Input R, input resistance; Insp Amp, inspiratory drive current amplitude; Physo, physostigmine; sEPSC Amp, sEPSC amplitude; sEPSC Frq, sEPSC frequency; Vm, membrane voltage; XII nu, the hypoglossal nucleus; XIIn, the hypoglossal nerve roots; ∫XIIn, integrated XIIn activity

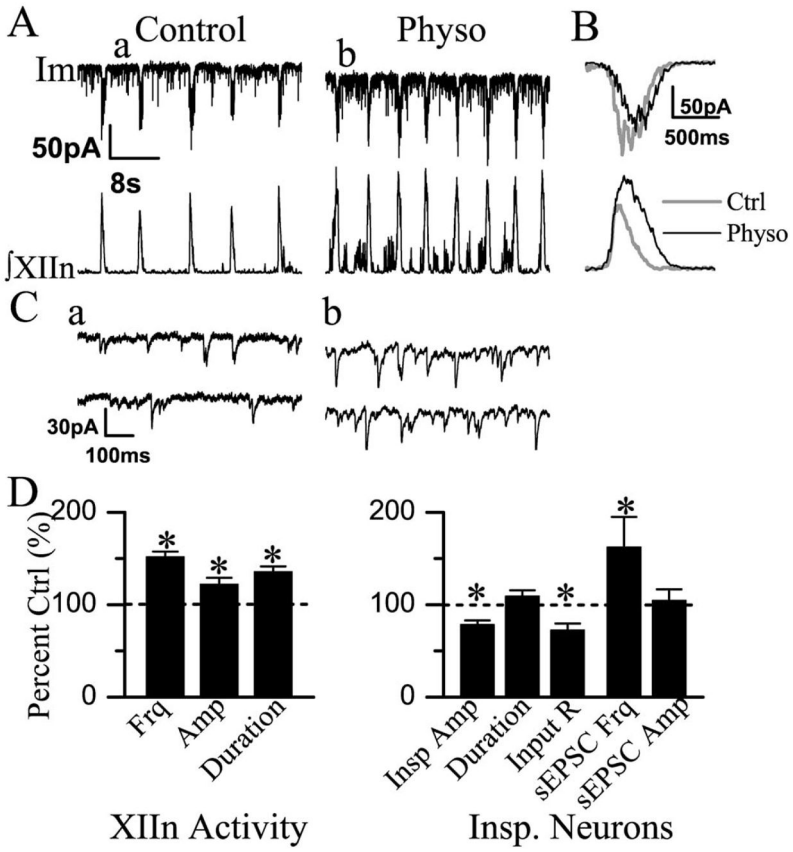

Fig. 3.

Bath application of Physo (10 μM) induced a tonic inward current, increased membrane noise, decreased the amplitude of phasic inspiratory drive current, increased the frequency of sEPSCs and decreased the input resistance in preBötC inspiratory neurons. Physo also increased respiratory frequency, the amplitude and duration of integrated inspiratory bursts of hypoglossal nerve. (A) Im, membrane current of inspiratory neuron voltage-clamped at −65 mV. (B) Phasic inspiratory drive current of an inspiratory neuron voltage-clamped at −65 mV in Ctrl and Physo conditions. Each trace was an average of five consecutive inspiratory periods triggered by the upstroke of the integrated inspiratory bursts from XIIn and the Im trace was low-pass filtered at 20 Hz. (C) sEPSCs during expiratory periods on an extended time scale; a and b correspond to the times labeled a and b in panel A. (D) Summary of the effects of Physo on XIIn rhythmic activity and on inspiratory neurons (mean±S.E.). The parameters of XIIn rhythmic activity include Frq, Amp and duration of integrated inspiratory bursts. The parameters of inspiratory neurons include Insp Amp and duration, Input R, sEPSC Frq and sEPSC Amp. * Statistical significance during Physo application vs. pre-Physo control (paired *t*-test). Numbers of neurons (*n*) for every experiment are indicated in the text of Results section.

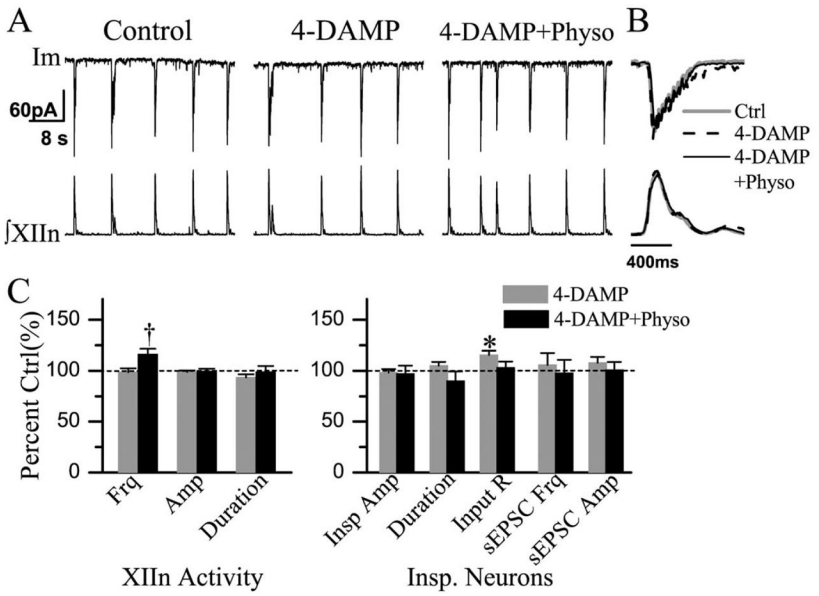

Fig. 4.

Bath application of 4-DAMP (2 μM) partially blocked the effects of Physo (10 μM). Physo increased Frq in the presence of 4-DAMP. (A) Im: membrane current from a voltage-clamped (−65 mV) inspiratory neuron. (B) Phasic inspiratory drive current of an inspiratory neuron voltage-clamped at −65 mV in control (Ctrl), 4-DAMP and 4-DAMP+Physo conditions. Each trace was an average of five consecutive inspiratory periods triggered by the upstroke of the integrated inspiratory bursts from XIIn and the Im trace was low-pass filtered at 20 Hz. (C) Summary of the effects of 4-DAMP, 4-DAMP+Physo on XIIn rhythmic activity and on inspiratory neurons (mean±S.E.). * Statistical significance during 4-DAMP application vs. pre-drug control. † Statistical significance during Physo application in the presence of 4-DAMP vs. 4-DAMP only conditions (one-way repeated measures ANOVA followed by post hoc comparison analyses based on Tukey). Numbers of neurons (*n*) for every experiment are indicated in the text of Results section.

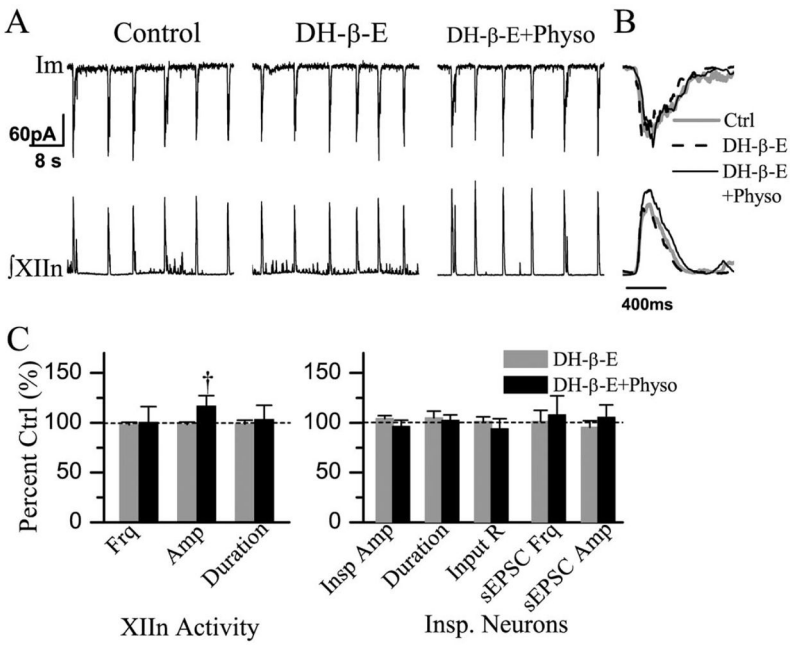

Fig. 5.

Bath application of DH-β-E (0.2 μM) partially blocked the effects of Physo (10 μM). Physo increased the amplitude of integrated inspiratory bursts of XIIn in the presence of DH-β-E. (A) Im:membrane current from a voltage-clamped (−65 mV) inspiratory neurons. (B) Phasic inspiratory drive current of an inspiratory neuron voltage-clamped at −65 mV in control (Ctrl), DH-β-E and DH-β-E+Physo conditions. Each trace is an average of five consecutive inspiratory periods triggered by the upstroke of the integrated inspiratory bursts from XIIn and the Im trace was low-pass filtered at 20 Hz. (C) Summary of the effects of DH-β-E, DH-β-E+Physo on ∫XIIn and on inspiratory neuron. † Statistical significance during Physo application in the presence of DH-β-E vs. DH-β-E only conditions (one-way repeated measures ANOVA followed by post hoc comparison analyses based on Tukey). Numbers of neurons (*n*) for every experiment are indicated in the text of Results section.

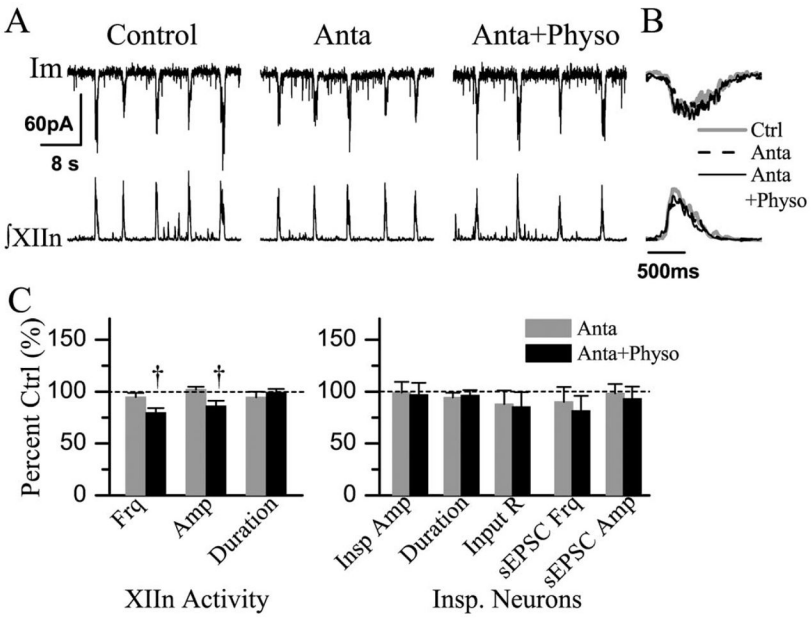

Fig. 6.

Bath application of 4-DAMP (2 μM) together with DH-β-E (0.2 μM) completely blocked the effects of Physo (10 μM). In the presence of antagonists 4-DAMP + DH-β-E (Anta), Physo decreased frequency and amplitude of respiratory-related rhythmic XIIn motor output. (A) Im: membrane current from a voltage-clamped (−65 mV) inspiratory neuron. (B) Phasic inspiratory drive current of an inspiratory neuron voltage-clamped at −65 mV in Ctrl, Anta and Anta +Physo conditions. Each trace is an average of five consecutive inspiratory periods triggered by the upstroke of the integrated inspiratory bursts from XIIn and the Im trace was low-pass filtered at 20 Hz. (C) Summary of the effects of Anta, Anta +Physo on XIIn rhythmic activity and on inspiratory neurons. † Statistical significance during Physo application in the presence of 4-DAMP and DH-β-E vs. Anta conditions (one-way repeated measures ANOVA followed by post hoc comparison analyses based on Tukey). Numbers of neurons (*n*) for every experiment are indicated in the text of Results section.

Table 1

Effects of 4-DAMP and its actions on the physostigmine-induced responses[a]

	Control	4-DAMP	4-DAMP+ physostigmine
XIIn rhythmic activity			
Frequency, min^{-1}	7.03±1.05	6.87±0.57	8.40±2.0†
Insp. amplitude (integrated), μV	22.0±11.6	21.8±11.7	20.9±12.4
Insp. duration, ms	519±101	483±96	504±111
preBötC neurons			
Insp. drive current amplitude, pA	−56.0±41.9	−56.4±44.3	−69.4±51.0
Insp. drive current duration, ms	667±217	699±246	542±124
Input resistance, MΩ	260.6±118.7	297.4±128.7*	292.4±175.1
Action potential threshold, mV	−53.7±3.2	−54.1±3.6	−54.0±3.9
sEPSC frequency, s^{-1}	3.04±1.67	3.05±1.50	3.04±1.41
sEPSC amplitude, pA	−18.3±6.92	−19.7±7.77	−20.9±8.07

Input resistance was measured using 30–50 pA 200 ms hyperpolarizing current pulses which caused 5–15 mV voltage step response. The frequency of sEPSCs is the number of sEPSCs divided by total expiration time during approximately 1–2 min recording time. Please refer to the Experimental Procedures and Results sections for the statistical tests for frequency and amplitude of sEPSCs. Numbers of neurons (*n*) for every experiment are indicated in the text of Results.

[a] Values are means±S.D. Respiratory frequency was taken as the reciprocal of the average of 10 consecutive respiratory periods in each condition for each preparation and was averaged across preparations. Inspiratory amplitude, duration, phasic inspiratory drive current amplitude and duration were measured from the averaged envelope of five consecutive inspiratory periods triggered by the upstroke of the integrated inspiratory bursts from XIIn for each condition. Durations were measured at 20% of peak amplitude.

* Statistically significant difference between 4-DAMP (2 μM) application vs. control conditions.

† Statistically significant difference between 10 μM physostigmine application in the presence of 4-DAMP vs. 4-DAMP alone conditions.

Table 2

Effects of DH-β-E and its actions on the physostigmine-induced responses[a]

	Control	DH-β-E	DH-β-E+ physostigmine
XIIn rhythmic activity			
Frequency, min^{-1}	7.72±2.16	7.57±2.17	7.01±1.44
Insp. amplitude (integrated), μV	20.9±13.0	20.7±13.2	28.2±20.0[†]
Insp. duration, ms	525±119	517±131	513±121
preBötC neurons			
Insp. drive current amplitude, pA	−62.5±46.4	−62.7±43.2	−69.6±54.8
Insp. drive current duration, ms	691±140	717±154	646±120
Input resistance, MΩ	294.9±132.0	306.7±172.4	273.6±138.7
Action potential threshold, mV	−51.9±3.4	−52.5±3.8	−53.4±4.4
sEPSC frequency, s^{-1}	2.75±1.40	2.83±1.86	3.29±3.10
sEPSC amplitude, pA	−12.5±2.6	−11.9±3.6	−12.5±5.7

[a] Values are means±S.D.

[†] Statistically significant difference between 10 μM physostigmine application in the presence of DH-β-E (0.2 μM) vs. DH-β-E alone conditions.

Table 3

Effects of 4-DAMP together with DH-β-E and their actions on the physostigmine-induced responses[a]

	Control	4-DAMP and DH-β-E	4-DAMP and DH-β-E+ physostigmine
XIIn rhythmic activity			
Frequency, min^{-1}	7.76±2.86	7.36±2.63	6.17±2.16[†]
Insp. amplitude (integrated), μV	18.4±8.3	18.5±7.9	15.8±7.9[†]
Insp. duration, ms	595±207	548±123	587±184
preBötC neurons			
Insp. drive current amplitude, pA	−34.6±18.4	−36.3±27.5	−33.5±22.7
Insp. drive current duration, ms	775±105	746±115	755±129
Input resistance, MΩ	248.9±101.3	235.0±41.6	243.1±27.9
Action potential threshold, mV	−52.9±5.14	−51.3±6.43	−52.2±6.94
sEPSC frequency, s^{-1}	3.17±2.0	3.22±2.87	3.01±2.84
sEPSC amplitude, pA	−16.78±6.53	−16.23±6.74	−15.39±7.24

[a] Values are means±S.D.

[†] Statistically significant difference between 10 μM physostigmine application in the presence of 4-DAMP (2 μM) and DH-β-E (0.2 μM) vs. 4-DAMP and DH-β-E conditions.